

NPS ARCHIVE
1965
MCCLOSKEY, T.

A DIAGNOSTIC STUDY AT 100MB OF THE
ZONALLY-AVERAGED FIELDS OF HEAT STORAGE,
HEAT TRANSPORT AND DIABATIC HEATING IN
THE NORTHERN HEMISPHERE DURING
EARLY APRIL 1963

TERRY J. McCLOSKEY.

A DIAGNOSTIC STUDY AT 100MB OF THE
ZONALLY-AVERAGED FIELDS OF HEAT STORAGE,
HEAT TRANSPORT AND DIABATIC HEATING IN
THE NORTHERN HEMISPHERE DURING EARLY
APRIL 1963

* * * * *

Terry J. McCloskey

A DIAGNOSTIC STUDY AT 100MB OF THE
ZONALLY-AVERAGED FIELDS OF HEAT STORAGE,
HEAT TRANSPORT AND DIABATIC HEATING IN
THE NORTHERN HEMISPHERE DURING EARLY
APRIL 1963

by

Terry J. McCloskey
//
Lieutenant, United States Navy

Submitted in partial fulfillment of
the requirements for the degree of

MASTER OF SCIENCE
IN
METEOROLOGY

United States Naval Postgraduate School
Monterey, California

1 9 6 5

NPS ARCHIVE

~~MT76~~

1965

MCCLOSKEY, T.

A DIAGNOSTIC STUDY AT 100MB OF THE
ZONALLY-AVERAGED FIELDS OF HEAT STORAGE,
HEAT TRANSPORT AND DIABATIC HEATING IN
THE NORTHERN HEMISPHERE DURING EARLY
APRIL 1963

by

Terry J. McCloskey

This work is accepted as fulfilling
the thesis requirements for the degree of

MASTER OF SCIENCE

IN

METEOROLOGY

from the

United States Naval Postgraduate School

ABSTRACT

The diabatic heating rate at 100mb is determined from the thermodynamic equation, utilizing previous calculations of the potential function χ and the "vertical velocity" ω , for the period 1-5 April 1963. The four basic terms of the expanded thermodynamic equation; storage, stream-velocity, χ -potential advection, and vertical heat transport are examined individually, and added to obtain \dot{Q} , the diabatic heating rate which is compared to the results of previous investigations. The zonally-averaged heating rates are discussed in terms of stratosphere circulations and their associated physical mechanisms.

ACKNOWLEDGMENT

The author is deeply indebted to Professor Frank L. Martin for his advice and guidance during the progress of the investigation. Appreciation is expressed to the author's wife, Mary Ann McCloskey, for her inspiration and for her part in typing the rough draft of the paper. Appreciation is also expressed to Mrs. Pat Johnson for her very able assistance in the programming and preparation of data for this investigation.

TABLE OF CONTENTS

Section	Title	Page
1.	Introduction	1
2.	The diabatic equation	2
3.	The irrotational wind and vertical motion structure	5
4.	Results	7
5.	Conclusions - stratospheric circulations and associated physical mechanisms	18
6.	Bibliography	25

LIST OF TABLES

Table		Page
1.	Zonally-averaged storage rates at 100mb for period one through nine (1-5 April 1963), in units 10^{-4} gpm sec $^{-1}$	12
2.	Zonally-averaged stream-velocity heat transport at 100mb for periods one through nine (1-5 April 1963), in units 10^{-3} gpm sec $^{-1}$	13
3.	Zonally-averaged χ -potential advection at 100mb for periods one through nine (1-5 April 1963), in units 10^{-3} gmp sec $^{-1}$	14
4.	Zonally-averaged vertical heat transport at 100mb for periods one through nine (1-5 April 1963), in units 10^{-1} gpm sec $^{-1}$	15
5.	Zonally-averaged diabatic heating rates at 100mb for periods one through nine (1-5 April 1963), in units 10^{-1} gpm sec $^{-1}$	16
6.	(a) 24-hour averages of storage, ψ -advection, χ -advection, vertical heat transport, and their contributions to the daily diabatic heating, averaged meridionally.	17
	(b) Comparison of \dot{Q} of this study with those of Davis [1].	17

LIST OF ILLUSTRATIONS

Figure	Page
1. The boundary conditions	6
2. Finite-differencing grid	6
3. Example of printout of \dot{Q} values (06 GMT, 1 April 1963)	9
4. Proposed meridional flow patterns early in spring-reversal period	20
5. 100mb height changes, April 1963 - April 1962 from analyses of the Free University of Berlin	22
6. 100mb analyses, 00 GMT, 1 April 1963 from analyses of the Free University of Berlin	23

TABLE OF SYMBOLS

c_p	- specific heat of air at constant pressure
d	- distance between successive grid points
D	- $z - z_p$ deviation from standard atmospheric height
f	- Coriolis parameter
g	- acceleration of gravity (980 cm sec^{-2})
gm	- gram
GMT	- Greenwich mean time
gpm	- geopotential meter
$J(A,B)$	- Jacobian of A and B, defined as $\frac{\partial A}{\partial x} \frac{\partial B}{\partial y} - \frac{\partial A}{\partial y} \frac{\partial B}{\partial x}$
K_n	- regression coefficients, $n=0, 1, 2$ in height extrapolation formula
\ln	- natural logarithm
ly	- langley
m	- map factor such that true distance = $m \times$ map distance
NCAR	- National Center for Atmospheric Research, Boulder, Colorado
\dot{Q}	- diabatic heating rate of a parcel
R_d	- gas constant for dry air
T	- temperature
t	- time
x	- x direction
y	- y direction
\hat{k}	- unit vector in the vertical
θ	- potential temperature
χ	- potential function
η	- vorticity

φ	- latitude
σ	- stability parameter, $-\frac{1}{\theta} \frac{\partial \theta}{\partial p}$
z	- $z(p)$ height of a pressure surface
z_p	- height of a pressure surface in the standard atmosphere
∇	- horizontal wind vector
∇	- $i \frac{\partial}{\partial x} + j \frac{\partial}{\partial y}$, the del operator
$\nabla \times$	- $\nabla \times$ irrotational component of the wind vector
$\nabla \psi$	- $\nabla \times \nabla \psi$ "stream" or non-divergent component of the wind
ω	- dp/dt vertical motion of the parcel in pressure co-ordinates
∇	- finite difference del operator
∇^2	- $\frac{\partial^2}{\partial x^2} + \frac{\partial^2}{\partial y^2}$, the del-squared operator
$\frac{d}{dt}$	- three dimensional parcel derivative operator
$\partial/\partial A$	- first partial derivative with respect to A
$\partial^2/\partial A^2$	- second partial derivative with respect to A
$[]$	- zonal average
$[]'$	- deviation from the mean zonal average
$\overline{[]}$	- area average of $[]$
a	- radius of earth, 6371 km
"B.R."	- an abbreviation for Balance Requirements per gram, $\dot{Q} - c_p \left(\frac{\partial T}{\partial t} \right)_p$

1. Introduction

There has been recent interest in the diabatic heating rates and related energy changes in the upper troposphere and lower stratosphere, notably by Davis [1], Julian [2], Martin [4], K. Myakoda [3], and others. Diabatic heating is, of course, also at the heart of the problem of large-scale energetics. However, the usual approach through energetics yields average values for a hemisphere for the period of study, whereas the approach of this study takes the more direct route of obtaining 12-hour average heating rates at each point of the usual octagonal (51 by 47) analysis-prediction grid system employed by the Joint Numerical Weather Prediction Unit, and other groups forecasting large-scale weather changes.

Martin [4] demonstrated the feasibility of the grid-point approach by obtaining 12-hour mean values of both the potential function χ of the wind and the "vertical velocity" $\omega = \frac{dp}{dt}$. Once these fields are known it is possible, utilizing the thermodynamic equation, to solve for \dot{Q} , the diabatic heating rate. Martin's model is described in his paper [4] and only those aspects required for this paper will be reviewed here. For more details regarding Martin's model, the reader is referred to his paper.

The data period selected for the calculations was 1-5 April 1963. The data was provided by the Joint Numerical Weather Prediction Unit, Washington, D.C. This particular data period was selected in an effort to reflect the relatively large heating rates and the associated large meridional flows that normally occur during April, particularly in the polar stratosphere.

2. The diabatic equation

If one expands the equation of thermodynamics, the result

$$\frac{I}{\Theta} \frac{d\Theta}{dt} = \frac{\partial I}{\partial t} + \nabla_{\psi} \cdot \nabla T + \nabla_{\rho} \chi \cdot \nabla T + \frac{I}{\Theta} \frac{\partial \Theta}{\partial p} \omega = \frac{\dot{Q}}{c_p} \quad (1)$$

follows. Here \dot{Q} is the heating rate per gram, while ψ and χ give the nondivergent and irrotational parts of the wind in accordance with:

$$\nabla = \mathbf{k} \times \nabla \psi + \nabla \chi$$

Here the fields of ψ and χ were obtained preliminarily by Martin [4] by solution of the Balance Equation, and the χ -2 equation respectively (see section 3). When the equation of state and hydrostatic equation are employed in (1), we obtain our basic working equation:

$$\frac{\partial}{\partial t} \left(\frac{-g}{R_d} \frac{\partial z}{\partial p} \right) + \nabla_{\psi} \cdot \nabla \left(\frac{-g}{R_d} \frac{\partial z}{\partial p} \right) + \nabla_{\rho} \chi \cdot \nabla \left(\frac{-g}{R_d} \frac{\partial z}{\partial p} \right) + \frac{I}{\Theta} \frac{\partial \Theta}{\partial p} \omega = \dot{Q}/c_p \quad (2)$$

The fourth term of (2) may be transformed into the more convenient form:

$$\begin{aligned} -\sigma \omega &= \frac{g}{R_d} \omega \frac{\partial z}{\partial p} \left(1 - \frac{R_d}{c_p} + \frac{\frac{\partial z}{\partial p}}{\frac{\partial \ln p}{\partial p}} \right) \\ &= \frac{g}{R_d} \omega^{(100)} \frac{\partial z}{\partial p} \left[.71296 + \frac{\left(\frac{\Delta z}{\Delta p} \right)_u - \left(\frac{\Delta z}{\Delta p} \right)_l}{\frac{1}{2} \ln \frac{3}{5} \left(\left[\frac{\Delta z}{\Delta p} \right]_u + \left[\frac{\Delta z}{\Delta p} \right]_l \right)} \right] \end{aligned} \quad (3)$$

where $\sigma = -\frac{I}{\Theta} \frac{\partial \Theta}{\partial p}$ but is also the negative of the coefficient of ω in the final form of (3). Here $\left(\frac{\Delta z}{\Delta p} \right)_u$ and $\left(\frac{\Delta z}{\Delta p} \right)_l$ are centered at 75mb and 125mb respectively, that is, at the upper-half and lower-half layer centers, respectively. The term $-\sigma$ of (3) has a positive sign since both $\partial z / \partial p$ and the contents of the last bracket are negative. This agrees with the intuitive expectation that an updraft ($\omega < 0$) is associated with vertical-motion cooling.

The factor $\partial z / \partial \ln p$ is present in all terms on the left side of (2),

and in order to determine its value at 100mb, the 50mb and 150mb data levels must be utilized. Unfortunately there was no vertically consistent 50mb data in punched-card form immediately available, so it was necessary to derive the 50mb contour data completely from regression equations. In order to do this the United States Navy Weather Research Facility Regression equations of D. Lea [5] were used. These equations have the following form:

$$Z_{50} = K_0 + K_1(Z_{100}) + K_2(T_{100}) \quad (4)$$

where K_0 , K_1 , K_2 represent the regression coefficients. It should be noted that the regression coefficients K_0 , K_1 , K_2 are listed by ten degree latitude bands from ten degrees north to the pole. It was necessary, therefore, to devise a computer program converting each $K_n(\psi)$ to a value of $K_n = K_n(i,j)$ defined at each grid point within the 51 by 47 octagon. This conversion was based upon a subprogram giving $\sin \psi$ in terms of the (i,j) grid. In addition $K_n(\psi)$ was made continuous with respect to latitude by averaging the values across the defining latitude boundaries for each ten degree band, while retaining the latitude-band mean value.

Since the 100mb contour analyses during the period of study were considered to be geographically consistent, whereas, those of temperature were not, it was decided again to obtain T_{100} using $T_{100} = -\frac{\partial Z}{\partial \ln p}$ in (4). With this modification, the regression equation is expressible in the following form:

$$(Z_{50} - Z_{100})^* = \frac{K_0 + K'_1(Z_{100}) + K'_2(Z_{100} - Z_{150})}{1 - K'_2} \quad (5)$$

where

$$K_1' = (K_1 - 1)$$

$$K_2' = K_2 \left(\frac{g}{R_d \ln 3} \right)$$

$$(z_{50} - z_{100})^* = \text{estimated thickness of the layer 100 to 50mb.}$$

and the term $\partial z / \partial \ln p$ appearing in (2) has been expressed in the form:

$$\frac{\partial z}{\partial \ln p} = - \frac{(z_{50} - z_{100})^* + (z_{100} - z_{150})}{\ln 3} \quad (6)$$

In (5) and (6), $(z_{50} - z_{100})^*$ is estimated from the modified regression equation (5), with input data z_{100} and $(z_{100} - z_{150})$ obtained from copies of data tapes provided by the Joint Numerical Weather Prediction Unit. The parameters z_{100} and $(z_{100} - z_{150})$ of (5) and (6) were used wherever possible in order to utilize as much vertically consistent data as possible, thereby tending to minimize errors due to the use of the regression equations (4) or (5). All computations were performed using the CDC 1604 computer.

Equation (3) can now be written in its final form:

$$\begin{aligned} & C_p \left(\frac{g}{R_d} \right) \frac{\partial}{\partial t} \left[\frac{(z_{50} - z_{100})^* + (z_{100} - z_{150})}{\ln 3} \right] + C_p \left(\frac{g}{R_d} \right) J(\psi) \left[\frac{(z_{50} - z_{100})^* + (z_{100} - z_{150})}{\ln 3} \right] \\ & C_p \left(\frac{g}{R_d} \right) \nabla_p \chi \cdot \nabla \left[\frac{(z_{50} - z_{100})^* + (z_{100} - z_{150})}{\ln 3} \right] - \frac{g_c}{R_d} \frac{\omega^{(100)}}{p_{100}} \left[\frac{(z_{50} - z_{100})^* + (z_{100} - z_{150})}{\ln 3} \right] \chi \quad (7) \\ & \left[.71296 + \frac{2}{\ln 3} \left(\frac{(z_{50} - z_{100})^* - (z_{100} - z_{150})}{(z_{50} - z_{100})^* + (z_{100} - z_{150})} \right) \right] = \dot{Q} \end{aligned}$$

It should be noted that $z = D + z_p$ where z_p is the standard atmosphere height and $D = z - z_p$ is the height anomaly relative to that of the standard atmosphere. In the first three terms of (7) z_p is independent

of the variables x, y, t so that the time and space derivatives become simply:

$$\frac{d}{dt} \left[(D_{50} - D_{100})^* + (D_{100} - D_{150}) \right], \quad \nabla \left[(D_{50} - D_{100})^* + (D_{100} - D_{150}) \right],$$

etc., and hence \bar{z}_p can be omitted. However this cannot be done in the vertical motion term where \bar{z}_p affects the vertical stability.

3. The irrotational wind and vertical motion structure.

As pointed out in section 1, the development in this section follows Martin [4], who solves diagnostically for χ for his χ -2 equation which is written:

$$\nabla^2 \hat{\chi}_{ij}^{(n)} = \frac{1}{\eta_{ij}} \left[f_1 \nabla^2 \hat{\chi}_{ij}^{(1)} - K \nabla \eta_{ij} \cdot \nabla \hat{\chi}_{ij}^{(n-1)} \right], \quad \hat{\chi} \equiv \chi / \frac{g}{f_1} \quad (8)$$

This equation is solved by relaxation using an iterative, scan-procedure, subject to the convergence requirement:

$$\left| \hat{\chi}_{ij}^{(n)} - \hat{\chi}_{ij}^{(n-1)} \right| \leq 4.0 \text{ cm}$$

Then with $\hat{\chi}$ assumed to be known, one may compute

$$\nabla \cdot \nabla \text{ or } \frac{g}{f_1} \nabla^2 \hat{\chi} = - \left(\frac{\partial \omega}{\partial p} \right) \quad (9)$$

Using $\omega = \omega(p)$, as a cubic polynomial in p , with an upper boundary condition $\omega = 0$ at $p = 0$, Martin also derives an integrated form of (9) giving $\omega = \omega^{(100)}$ at each grid point.

In terms of finite difference notation $\omega^{(100)}$ has been shown [4] to be:

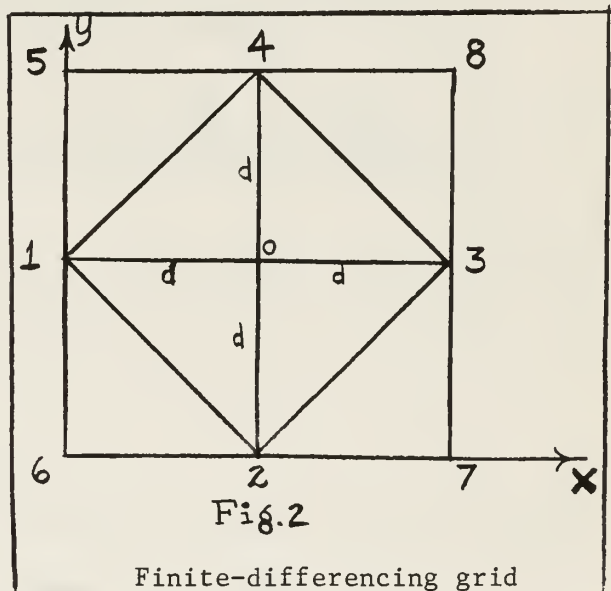
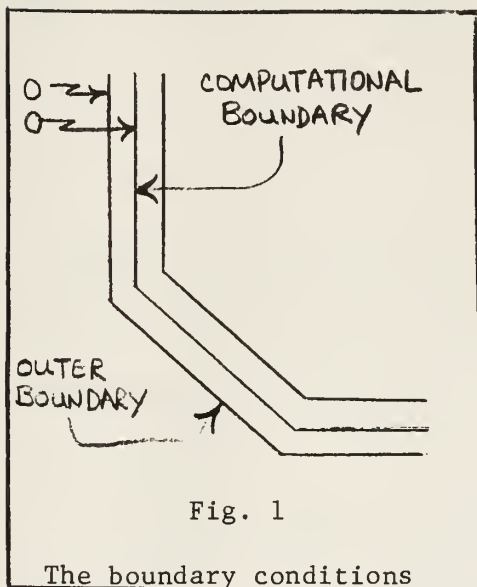
$$\omega_{ij}^{(100)} = -1.5 \frac{g}{f_1} \nabla^2 \hat{\chi}_{ij} \quad (10)$$

Here $\hat{\chi}$ is scaled in terms of centimeters, as this scaling was defined

is (8). From (10), $\omega_{ij}^{(100)}$ takes on the finite difference form:

$$\omega_{ij}^{(100)} = -\frac{3}{2} \frac{g}{f_1} \frac{m^2}{d^2} \nabla^2 \hat{\chi}_{ij} \quad (11)$$

with $\hat{\chi}_{ij}$ assumed zero on the two outermost rows of the octagon. This was also the boundary condition used by Martin in solving (8). The 47 by 51 octagonal grid mapping program used in the computations was furnished on tapes by the National Center for Atmospheric Research. Since it is not possible to compute $\nabla^2 \chi$ on the "outer boundary" (Fig. 1), it was necessary to set $\omega = 0$ on the outer boundary throughout the computations.



The normal five-point map grid 1-2-3-4-0 was used one row within the computational boundary, while a nine-point grid was used at all points further inside. The nine-point grid simply inserts a three-point mean for a normal difference; for example, the $\chi_3 - \chi_1$ difference of a five-point grid is replaced with the weighted difference:

$$[(\chi_8 - \chi_5) + 2(\chi_3 - \chi_1) + (\chi_7 - \chi_6)] / 4$$

in the nine-point grid. The actual five-point finite-differencing

schemes used in the computations are as follows, relative to terms in Eq. 7:

$$\frac{\partial}{\partial t} \left(\frac{\partial Z}{\partial \ln p} \right)_t = \frac{1}{2\Delta t} \left[\left(\frac{\partial Z}{\partial \ln p} \right)_{t+1} - \left(\frac{\partial Z}{\partial \ln p} \right)_{t-1} \right]$$

$$J_5 \left(\psi, \frac{\partial Z}{\partial \ln p} \right) = \frac{1}{4(d^2/m^2)} \left\{ (\psi_3 - \psi_1) \left[\left(\frac{\partial Z}{\partial \ln p} \right)_4 - \left(\frac{\partial Z}{\partial \ln p} \right)_2 \right] - \right. \\ \left. (\psi_4 - \psi_2) \left[\left(\frac{\partial Z}{\partial \ln p} \right)_3 - \left(\frac{\partial Z}{\partial \ln p} \right)_1 \right] \right\}$$

$$\nabla_p \chi \cdot \nabla \left(\frac{\partial Z}{\partial \ln p} \right) = \frac{1}{4(d^2/m^2)} \left\{ (\chi_3 - \chi_1) \left[\left(\frac{\partial Z}{\partial \ln p} \right)_3 - \left(\frac{\partial Z}{\partial \ln p} \right)_1 \right] + \right. \\ \left. (\chi_4 - \chi_2) \left[\left(\frac{\partial Z}{\partial \ln p} \right)_4 - \left(\frac{\partial Z}{\partial \ln p} \right)_2 \right] \right\}$$

Furthermore the resultant ω_{ij} from (11) have been smoothed twice everywhere interior to the two boundary rows just mentioned, giving $\bar{\omega}_{ij}$, the values used in this study.

4. Results

With the fields of χ_{ij} and $\bar{\omega}_{ij}$ known, as well as ψ_{ij} and observed values of

$$\frac{g}{R_d} \frac{\partial}{\partial t} \left[\frac{(Z_{50} - Z_{100})^* + (Z_{100} - Z_{150})}{\ln 3} \right]$$

from consecutive 12-hour map-fields, \bar{Q} has been determined from (7).

The first term of (7), called the "storage term" is

$$c_p \frac{\partial}{\partial t} \left\{ \frac{g}{R_d \ln 3} \left[(Z_{50} - Z_{100})^* + (Z_{100} - Z_{150}) \right] \right\} \quad (12)$$

The second and third terms represents the 12-hour mean horizontal heat-

transport at the gridpoint (i,j) and have the combined form:

$$\frac{g}{R_d \ln 3} \left\{ \underbrace{J(\psi, [(z_{50}-z_{100})^* + (z_{100}-z_{150})])}_{\text{"}\psi\text{-transport"}} + \underbrace{\nabla_p \chi \cdot \nabla [(z_{50}-z_{100})^* + (z_{100}-z_{150})]}_{\text{"}\chi\text{-transport"}} \right\} \quad (13)$$

The fourth term in (7) is the vertical heat transport (ω -transport)

$$-\frac{g(\omega)}{R_d \ln 3} \left[(z_{50}-z_{100})^* + (z_{100}-z_{150}) \right] \left(0.71296 + \frac{2}{\ln^{3/5}} \frac{[(z_{50}-z_{100})^* - (z_{100}-z_{150})]}{[(z_{50}-z_{100})^* + (z_{100}-z_{150})]} \right) \quad (14)$$

The four terms on the left side of (7), which have been listed in the preceding paragraph, have also been computed individually as functions of (i,j) everywhere within the computational boundary. Combined values have been formed to give resultant octagonal fields of $\dot{Q}(i,j)$. For a typical field of \dot{Q} see Fig. 3. Zonal-averages of each of the five fields have been computed by programming an averaging routine for each five degree latitude band (over an area of 20-90 degrees latitude).

\dot{Q} , and the preceding four terms as well, have units of gpm which, for later comparison purposes must be changed to langleys. \dot{Q} may be determined by a sum of terms of the form:

$$\dot{Q} = M_{100} \frac{c_p}{R_d \ln 3} \frac{\partial (g \Delta z)}{\partial t} = M_{100} \frac{c_p g}{R_d \ln 3} \frac{\partial (\Delta z)}{\partial t} \quad (15)$$

Here \dot{Q} is in $\text{ergs}(\text{gm})^{-1} (\text{sec})^{-1} \text{cm}^{-2}$ provided all terms on the right side of (15) are in c.g.s. units, $\Delta z = z_{50} - z_{150}$ in gp-cm and M_{100} = mass of

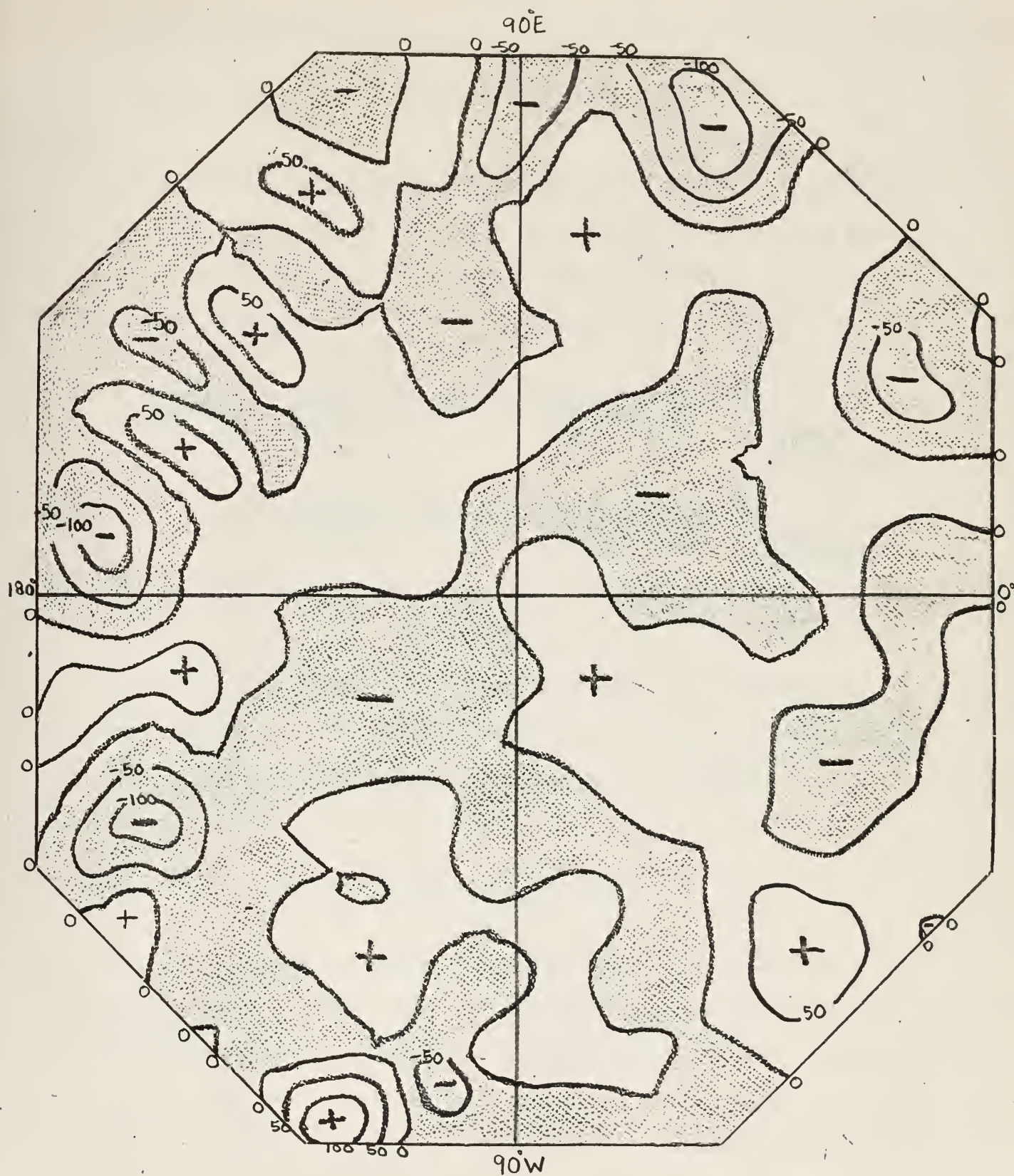


Fig. 3. Example of printout of Q values for (06 GMT, 1 April 1963)

the column 150mb to 50mb.

$$\dot{Q} = M_{100} \frac{c_p}{\ln 3} \left\{ 3.419 \times 10^{-4} \left(\frac{\partial}{\partial t} [\Delta Z_{gP-cm}] \right) \right\}_{gP-cm/sec} \quad (16)$$

The expression within the braces of (16) is now identical to $(\partial \bar{T} / \partial t)$ in units of $(^{\circ}K)(sec)^{-1}$. To get a corresponding value of \dot{Q} per gram per day, both sides of (16) are multiplied by $86,400 \text{ sec (day)}^{-1}$ and divided by 102, the latter being the number of gms in 100mb:

$$\begin{aligned} \dot{Q} \left(\frac{\text{ly}}{\text{gm day}} \right) &= \frac{c_p}{\ln 3} \left[3.419 \times 10^{-2} \times \frac{86,400}{102} \right] \left[\frac{\partial}{\partial t} (\Delta Z) \right]_{gPM/sec} \\ &= \frac{.239}{1.0986} \left[3.419 \times 10^{-2} \times \frac{86,400}{102} \right] \left[\frac{\partial}{\partial t} (\Delta Z) \right]_{gPM/sec} \end{aligned}$$

$$\dot{Q} = 6.298 \times \left[\frac{\partial}{\partial t} (\Delta Z_{gpm}) \right] \dots \text{ly (gm)}^{-1} (\text{day})^{-1}$$

The units of $\partial / \partial t [\Delta Z]$ are emphasized as gpm (sec)^{-1} because this is the form of the computer output units. Thus it follows from $\left[\partial (\Delta Z) / \partial t \right]$ that a geopotential change of $1 \text{ gpm (gm)}^{-1} \text{sec}^{-1}$ is equivalent to a heating rate of:

$$6.298 \text{ ly (gm)}^{-1} (\text{day})^{-1}$$

The last statement is typical of each of the terms in (12), (13), (14). Zonal averages for each term and their zonal mean sum $[\dot{Q}]$ of (7) have been determined and are listed by latitude belts in Tables 1 through 5. This is done also, for purposes of comparison, with computations of $[\dot{Q}]$ made by Davis [1], who used a climatological or standardized atmosphere (Table 6). Note that the notation $[]$ indicates a zonal average at a

specified latitude.

In Table 6, the nine sets of results obtained here are averaged to give a mean daily average of the storage, the horizontal transport terms of both the stream and potential types, the vertical-heat transport and the resultant \dot{Q} , each in $\text{ly}(\text{gm})^{-1} \text{ day}^{-1}$. Davis' results have been centered at 117.5mb, but presumably this slight shift of levels is insignificant. In regard to the units of $\text{ly}(\text{mb})^{-1} \text{ day}^{-1}$ attributed to Davis, it should be recalled that

$$1 \frac{\text{ly}}{\text{mb}} = \frac{1 \text{ cal}}{1000 \text{ dynes}}$$

whereas our unit of heat is:

$$1 \frac{\text{ly}}{\text{gm}} = \frac{1 \text{ cal}}{980 \text{ dynes}}$$

Thus the two heating rates, of this paper and of Davis, are very nearly compatible. The essential results are presented here as meridional cross-sections contained in Tables 1 through 6.

In Table 6b, Davis' computations for mean daily \dot{Q} are based upon a climatological atmosphere at rest. It will be seen that \dot{Q} should depend upon the nature of the meridional motion pattern, especially the field of vertical motion, in addition to any static distribution of radiating material. The term "Balance" is taken from Davis' paper and refers to balance requirements, on the basis that

$$-(B.R.) = \dot{Q} = c_p [\mathbf{V}_\psi \cdot \nabla T + \mathbf{V}_\chi \cdot \nabla_p T - \sigma \omega]$$

with the "storage" very small (by several orders of magnitude) both in the present study and in Davis'.

LAT PRD	50-45	45-40	40-35	35-30	30-25	25-20	55-50
	90-85	85-80	80-75	75-70	70-65	65-60	60-55
1	3.813 4.098	19.552 5.067	21.829 2.714	23.257 1.464	20.797 1.013	10.836 -1.355	2.575 -1.168
2	-9.955 -5.752	-15.967 -2.396	-12.731 1.177	-8.024 2.922	-3.426 1.590	1.410 1.611	-6.590 -4.164
3	31.410 2.079	5.569 3.033	-15.807 1.352	-9.467 .552	.048 .811	-.108 .523	3.243 2.721
4	-27.531 1.573	-20.092 .206	-6.703 -3.247	-9.549 -2.047	-18.728 -.082	-17.029 .172	-6.309 .238
5	41.324 -.882	46.899 .281	37.409 .896	11.599 .179	5.813 -1.632	7.475 -1.320	.483 -1.542
6	-38.337 -2.380	-37.035 -1.082	-31.526 -1.159	-16.093 -1.675	-9.327 .436	-7.917 .466	-3.350 3.224
7	35.607 1.950	22.216 1.895	10.735 .194	-7.791 -1.013	-6.200 -2.906	-1.985 -1.565	.555 -3.428
8	-.417 2.847	-1.109 1.052	-3.120 1.411	-5.161 1.932	-2.242 .705	-3.298 -.195	-3.943 -.971
9	11.359 1.694	17.853 3.529	19.209 1.311	15.865 -5.516	5.183 -.134	-1.890 .427	-5.071 -3.866
9-PRD TOTALS	47.274 5.227	37.886 8.854	19.296 4.649	1.637 1.798	-8.082 -1.155	-12.507 -1.234	-18.407 -7.955

Table 1. Zonally-averaged storage rates at 100mb for period one through nine (1-5 April 1963), in units of 10^{-4} gpm sec $^{-1}$ [Conversion factor for ly (gm) $^{-1}$ (day) $^{-1}$: 1 gpm sec $^{-1}$ = 6.2981y (gm) $^{-1}$ (day) $^{-1}$]

LAT PRD	50-45	45-40	40-35	35-30	30-25	25-20	55-50
	90-85	85-80	80-75	75-70	70-65	65-60	60-55
1	41.872 32.721	-2.832 -7.916	-9.557 -1.743	-38.930 8.894	-40.827 7.276	-5.333 -9.259	36.481 -16.954
2	14.491 7.394	-7.097 -7.371	-16.313 3.068	10.832 4.738	-71.656 1.137	30.664 -1.630	-3.083 -1.093
3	26.414 8.44C	9.511 -11.092	-9.558 3.064	-13.654 5.078	-13.446 2.50C	-14.439 1.652	13.067 -6.904
4	58.274 12.578	34.422 -17.996	-26.007 2.633	-36.430 11.043	6.679 .847	5.353 2.286	2.639 -15.034
5	65.951 1.112	4.760 -5.473	-21.589 3.344	-17.068 15.687	-44.067 4.792	-35.016 -4.924	56.896 -6.756
6	35.841 6.488	-1.250 -4.886	-13.334 5.358	-37.683 4.401	-16.657 .376	-91.406 -340	78.179 17.495
7	5.642 -8.008	-7.528 -2.856	-898 -112	-26.977 -2.981	17.805 7.30C	-91.254 -233	51.072 33.020
8	15.248 3.994	26.660 -3.696	-15.489 1.769	-65.007 -3.896	53.968 3.881	-110.658 4.844	77.732 17.113
9	57.316 .431	27.985 1.105	-33.150 3.052	-42.349 -10.494	61.935 6.792	-104.907 6.663	65.552 7.554
9-PRD TOTALS	321.050 65.149	84.631 -60.182	-145.895 20.433	-267.266 32.470	-46.267 34.902	-416.995 -939	378.536 28.441

Table 2. Zonally-averaged stream-velocity heat transport at 100mb for periods one through nine (1-5 April 1963), in units of 10^{-3} gpm sec⁻¹ [Conversion factor: 1 gpm sec⁻¹ = 6.2981y gm⁻¹ day⁻¹]

LAT PRD	50-45	45-40	40-35	35-30	30-25	25-20	55-50
	90-85	85-80	80-75	75-70	70-65	65-60	60-55
1	12.603 7.363	27.500 1.379	20.636 -7.08	2.754 -47.703	-72.871 -59.579	-99.182 -7.64	-53.090 -7.443
2	-4.57 6.643	6.323 1.158	43.470 4.185	55.370 31.093	46.327 3.211	-44.403 -1.333	-80.158 -12.318
3	-7.519 -29.314	-28.766 1.280	-33.092 -6.97	5.334 -21.431	29.562 -42.880	74.064 -3.494	60.403 -33.282
4	22.436 -14.993	56.788 -5.434	69.113 1.441	59.361 7.745	26.866 17.605	60.891 2.052	91.285 34.872
5	15.577 -14.286	25.084 .197	33.651 -1.434	12.461 -1.149	11.803 30.451	-45.332 5.291	-44.708 -25.789
6	10.445 -13.075	27.034 -.110	70.443 1.228	68.285 51.998	-1.481 98.065	-27.750 10.771	90.963 2.239
7	-5.198 11.121	-15.273 .361	26.184 -2.112	69.199 -27.465	26.275 -1.730	-111.770 1.758	-112.308 -4.595
8	8.471 .888	17.070 1.727	13.042 -6.13	1.083 6.815	3.602 -43.920	44.910 -4.763	-10.674 -47.760
9	-2.796 -15.072	-7.331 -7.355	-13.924 -4.221	12.628 -16.192	73.954 -16.092	63.275 .215	18.130 12.175
9-PRD TOTALS	53.562 -60.724	108.428 -6.797	229.523 -2.931	286.479 -15.288	144.035 -14.865	-85.297 9.734	-40.154 -81.900

Table 3. Zonally-averaged χ -potential advection at 100mb for periods one through nine (1-5 April 1963), in units of 10^{-3} gpm sec $^{-1}$ [Conversion factor: 1 gpm sec $^{-1}$ = 6.2981y gm $^{-1}$ day $^{-1}$]

LAT PRD	50-45	45-40	40-35	35-30	30-25	25-20	60-55	55-50
1	14.645 .231	4.508 2.244	-2.072 5.360	-3.821 3.529	-2.908 -9.606	-.282 -18.127	.137	-.247
2	3.698 -.09C	6.215 -1.097	4.570 -4.263	-.213 1.001	-3.214 6.179	-2.028 .206	-.087	-.182
3	-12.308 -1.616	-5.459 -.016	2.190 5.524	3.244 1.683	1.708 -3.127	.790 -14.577	-.459	.367
4	26.505 1.626	12.441 .797	1.493 -3.061	-2.065 -4.684	-1.131 1.400	1.256 16.643	.157	.580
5	9.860 -1.080	5.614 2.046	-.272 .289	-1.264 -7.392	-1.970 -2.444	-.812 3.261	-.261	.075
6	11.529 .411	10.499 .342	4.486 -7.950	-2.969 -12.409	-2.678 4.286	.863 25.067	.407	.399
7	-5.857 -.431	2.459 .351	7.871 5.575	.213 -1.023	-6.329 -5.737	-2.139 8.972	.018	-.369
8	6.261 -.77C	1.950 .034	-1.108 -2.020	-.574 6.288	1.490 4.016	-.115 -12.678	-.571	-.166
9	-2.255 1.148	-1.312 2.030	1.705 -.973	3.754 -.671	.543 -4.761	-.136 -12.115	-.193	.251
9-PRD TOTALS	52.078 -.57C	36.916 6.731	18.862 -1.519	-3.694 -13.677	-14.488 -9.795	-2.603 -3.347	-.852	.709

Table 4. Zonally-averaged vertical heat transport at 100mb for periods one through nine (1-5 April 1963), in units of 10^{-1} gpm sec $^{-1}$ [Conversion factor: 1 gpm sec $^{-1}$ = 6.2981y gm $^{-1}$ day $^{-1}$]

LAT PRD	50-45	45-40	40-35	35-30	30-25	25-20	60-55	55-50
1	15.064 .555	4.480 2.165	-2.168 5.342	-4.210 3.618	-3.316 -9.533	-3.336 -18.219	.502	-.416
2	3.843 -.016	6.144 -1.171	4.407 -4.233	-1.104 1.048	-3.930 6.190	-1.721 .190	-.118	-.193
3	-12.044 -1.531	-5.363 -.127	2.094 5.555	3.107 1.734	1.574 -3.102	.646 -14.560	-.328	.298
4	27.087 1.752	12.786 .617	1.233 -3.035	-2.430 -4.574	-1.064 1.409	1.309 16.666	.184	.430
5	10.520 -1.069	5.662 1.991	-.488 .323	-1.434 -7.235	-2.411 -2.397	-1.162 3.212	.308	.007
6	11.887 .475	10.486 .293	4.353 -7.896	-3.345 -12.365	-2.845 4.289	-.051 25.064	1.188	.574
7	-5.800 -.511	2.384 .323	7.862 5.574	-6.151 -1.053	-3.052 -5.664	8.970	.528	-.039
8	6.413 -.730	2.216 -.003	-1.263 -2.002	-1.224 6.250	2.030 4.054	-1.222 -12.629	.206	.005
9	-1.682 1.153	-1.032 2.041	1.373 -.943	3.330 -.776	1.163 -4.693	-1.186 -12.048	.463	.326
9-PRD TOTALS	55.288 .081	27.762 6.129	17.403 -1.315	-6.367 -13.353	-14.951 -9.446	-6.773 -3.356	2.933	.993

Table 5. Zonally-averaged diabatic heating rates at 100mb for period one through nine (1-5 April 1963), in units of 10^{-1} gpm sec $^{-1}$ [Conversion factor: 1 gpm sec $^{-1}$ = 6.2981y day $^{-1}$ gm $^{-1}$]

	20-25	25-30	30-35	35-40	40-45	45-50	50-55	55-60	60-65	65-70	70-75	75-80	80-85	85-90
$\rho/\sigma_t \times 10^{-2}$	-.01	+.00	.03	.06	.07	.02	-.08	-.17	-.16	-.08	.07	.28	.48	.57
$c_p \nabla \psi \cdot \nabla T$.01	.03	.03	-.00	-.01	.05	.13	.06	-.17	-.32	-.29	-.13	.09	.20
$c_p \nabla x \cdot \nabla T$	+.00	-.00	-.01	-.01	-.03	-.06	-.08	-.07	.01	.16	.29	.28	.19	.15
$-g \omega \sigma$	-.56	-1.02	-.95	-.41	.11	.24	.05	-.26	-.55	-.41	.63	2.49	4.48	5.20
BALANCE REQ	.55	.99	.93	.42	-.07	-.23	-.10	.27	.71	.57	-.63	2.64	4.66	5.54
$Q \frac{dy}{dy} \text{ gm}$	-.55	-.99	-.93	-.42	.07	.23	.10	-.27	-.71	-.57	.63	2.64	4.66	5.55

(a)

	20-25	25-30	30-35	35-40	40-45	45-50	50-55	55-60	60-65	65-70
$\rho/\sigma_t \times 10^{-1}$.03	.02	-.00	-.01	+.00	.04	.09	.15	.20	.26
SOLAR HEATING $H_2O \times 10^{-1}$.18	.18	.18	.18	.17	.16	.16	.15	.14	.13
SOLAR HEATING $O_3 \times 10^{-1}$.10	.12	.14	.16	.18	.20	.22	.23	.24	.25
INFILTRATION COOLING	.07	.10	.13	.15	.17	.19	.21	.22	.23	.24
BALANCE REQ	.06	.08	.09	.11	.13	.16	.19	.20	.22	.23
$Q \frac{dy}{dy} \text{ mb}$	-.04	-.07	-.09	-.11	-.14	-.15	-.16	-.17	-.18	-.19

(b)

Table 6. (a) 24-hour averages of storage, ψ -advection, x -advection, vertical heat transport and their contributions to the daily diabatic heating, averaged meridionally
(b) Comparison of Q of this study with those of Davis [1]

5. Conclusions: stratospheric circulations and associated physical mechanisms

As already noted, the zonally-averaged storage term is very small. In addition the stream- and potential-advections, averaged over five-degree latitude bands are smaller by approximately two orders of magnitude than $[\dot{Q}]$. Thus to a good approximation, valid everywhere at least as to sign,

$$[\dot{Q}] \doteq -c_p [\bar{\omega}]$$

and is of the proper order of magnitude as well.

By the equation:

$$[\omega_{100}] = -\frac{3}{2} \frac{g}{f} \frac{m^2}{a^2} [\nabla^2 \hat{\chi}_{100}] = -\frac{3}{2} [\nabla \cdot \nabla_{100}] \quad (17)$$

it follows that $[\omega_{100}] > 0$ occurs when $[\nabla \cdot \nabla]$ represents convergence.

Now convergence occurs near the pole, since the expression for the zonally-averaged divergence

$$[\nabla \cdot \nabla_{100}] = \left[\frac{\partial^2 \chi}{\partial y^2} \right] - \left[\frac{\partial \chi}{\partial y} \right] \frac{\tan \phi}{a} \quad (18)$$

with the second term (which represents the convergence of meridians)

becoming dominant [Martin, 4] at latitudes $\phi > 75N$. At lower latitudes

$$[\nabla \cdot \nabla_{100}] = [\nabla^2 \chi_{100}] \doteq [\partial^2 \chi / \partial y^2]$$

is a valid approximation; that is, the spherical divergence is only

slightly affected by convergence of meridians. Hence, where $[\omega_{100}]$ is

negative, there is divergence; if $[\omega_{100}]$ is positive, there is convergence.

Consequently at 100mb, we have centers of convergence at the pole and

latitude 35, and of divergence at latitude 65.

In inferring a stratospheric circulation, one may start with an interhemispheric meridional circulation proposed by Kellogg [6], especially applicable, in some of its aspects, to the winter-summer reversal in the stratosphere. The octagonal grid, together with the associated boundary conditions, is not able to resolve the effect of the cross-equatorial flow to at least latitude 20N latitude. However, because of the decrease of mass in the winter stratosphere, cross-equatorial flow must occur near the time of the vernal equinox. This evidently is responsible for the convergence center near latitude 35N.

Likewise with the return of the sun to the Northern Hemisphere, ozone regeneration goes on rapidly, followed by ozone-heating, especially at 45 km. According to Pressman [7], an ozone radiative heating maximum proceeds progressively from 30N latitude to the pole between the dates 15 March and 15 May. For time of this study, 1-5 April, 1963, one might expect maximum ozone heating at 45 km at or near 60N latitude. This effect is so marked as to cause a strong forced outdraft ($\nabla \cdot \mathbf{V} > 0$) at 60N latitude, and at an elevation of 45 km. In order that three-dimensional mass divergence be within reasonable bounds, there must be a sympathetic updraft from below. This is the $[\omega]$ measured at the 100mb level and presumably exists at levels between 100mb and 45km. Also according to Martin's model, sizeable ω -values of the same sign still persist at the 200mb level, but are smaller than ω_{100} in units of cm sec^{-1} . The level of "return flow" in these cells cannot be designated from presently known studies.

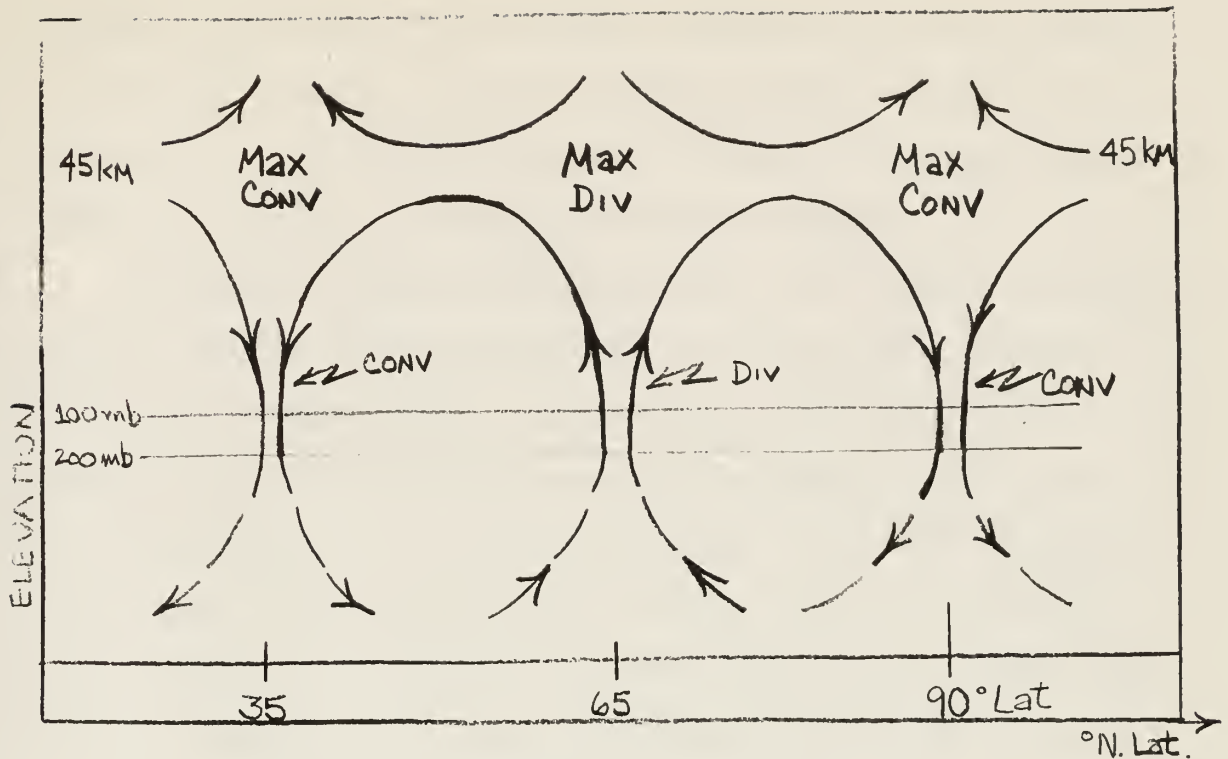


Fig. 4. Proposed meridional flow patterns early in the spring-reversal period

The "maximum" convergence in the vertical and associated downdrafts at the pole at this particular time of ozone activity should then be viewed as a "spill-over" effect from 65N latitude. The maximum convergence at or near latitude 35 North, which mirrors a zonally-averaged 100-mb maximum values of \bar{w} at this same latitude is postulated as the primary result of cross-equatorial flow. Considering the level at which the greatest polar-vortex intensification in the Southern Hemisphere occurs, the level of the 35N latitude maximum of convergence has also been placed at 45km.

Fig. 4 together with the above discussion "explains" the mean meridional flow pattern in the stratosphere during the period of this study. One may offer as conjecture that as the stratospheric summer

advances (say by June 15), the maximum convergence will have advanced to 45N latitude while the zone of maximum divergence associated with most effective ozone-heating near 45km advances to the pole, there to become associated with divergence at higher elevations.

As contrasted with the \dot{Q} of this study, Davis' results show only moderate cooling at every latitude due to predominance of long-wave radiation over heat sources. Two features by which April, 1963 appears to differ from climatology are shown in Figs. 5 and 6, both taken from analyses of the Free University of Berlin [8]. The latter figure shows a pre-existing zone of vortices at latitude 60 North, as of 1 April, 1963, 1200 GMT. The other figure mentioned above shows that, as compared with a completely different April (1962), pressure was higher over the pole but lower than in 1962 in a vortex ring at 60N latitude. Fig. 6 shows a possible reason for this: strong baroclinicity on the equatorward side of the vortices, with 'zonal generation'

$$G_z = \overline{\left(\frac{1}{\theta} \frac{\partial \theta}{\partial z}\right)}' \overline{[Q][T]}'$$

computed over 45-70 degrees North latitude favoring the continuation of such a baroclinic zone and westerly winds. In fact, according to the analyses of the Free University of Berlin, an easterly regime with an associated polar anticyclone did not occur until May 15, 1963.

Finally, how may one reconcile the zonally-averaged equation:

$$\dot{Q} - (-c_p \sigma w) \approx 0 \quad (19)$$

so that both horizontal flows and storage are relatively unimportant

Institut für Meteorologie
und Geophysik
der Freien Universität
Berlin

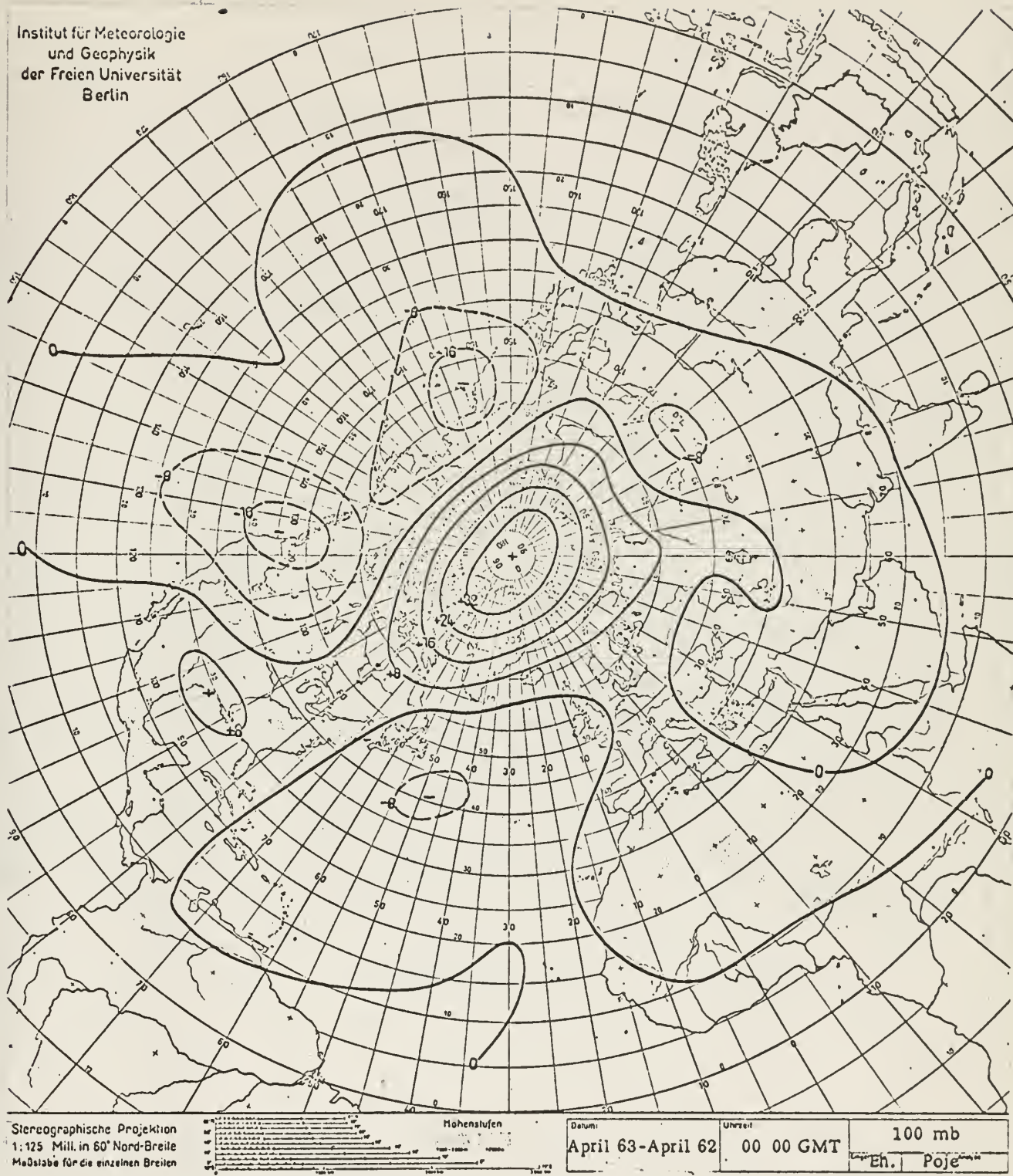


Fig. 5. 100mb height changes, April 1963 - April 1962 from analyses of the Free University of Berlin



Fig. 6 100mb analyses, 00GMT, 1 April 1963 from analyses of the Free University of Berlin

as determined here. Equation (19) implies that with $-c_p[\sigma\omega] > 0$ (down-draft motions), $[\dot{Q}] < 0$ is the result. Such a result is reasonable on physical grounds by noting that descending air is warmed dry adiabatically, and in addition one may expect some increased diabatic solar heating acting upon an ozone increase in lower stratospheric elevations. However, one immediate opposing result is that the CO_2 in the warmed air will emit at a greater rate, tending to re-establish the heat balance. The same argument applies in reverse for updraft motions.

BIBLIOGRAPHY

1. Davis, P. A. An analysis of the atmospheric heat budget. *Journal Atmospheric Sciences*, v. 20, Jan., 1963: 5-20.
2. Julian, P. R. Some aspects of tropospheric circulation during midwinter stratospheric warming events. *Journal Geophysical Research*, v. 70, n. 4, Feb., 1965: 757-767.
3. Miyakoka, K. Some characteristic features of winter circulation in the troposphere and lower stratosphere, Tech. Rept. 14. Department of Geophysical Sciences, University of Chicago. 1963.
4. Martin, F. L. A Diagnostic Method for Computing the 12-hour Mean Velocity Potential with Special Application to the Layer 100-300 mb National Center for Atmospheric Research Preprint n. 64-6(b), June, 1964.
5. Lea, D. Regression Equations for Vertical Extrapolation of Constant-Pressure-Surface Heights and Temperatures between 200mb and 30mb. Presented at AMS Meeting, Chicago, 1961.
6. Kellogg, W. W., Schilling, G. F. A proposed model of the circulation in the upper stratosphere. *Journal Meteorology*, v. 8, n. 4, Aug., 1951: 222-230.
7. Pressman, J. Seasonal and latitudinal temperature changes in the ozonosphere. *Journal Meteorology*, v. 12, n. 1, Feb., 1955: 87-89.
8. Scherhag, R., et al. Tagliche Höhenkarten der 100-mbar-Fläche sowie monatliche Mittelkarten für das Jahr 1963. *Meteorologische Abhandlungen*, Band XXXVII, Heft 2.

thesM176

A diagnostic study at 100 MB of the zona



3 2768 002 12330 9

DUDLEY KNOX LIBRARY